Enhancing edge chemistry in HCP-Ru catalysts through crystalline domain engineering for efficient alkaline hydrogen evolution

Shuai Zhao,[a] *Jie Xu,*[b] *Chang Wang,*[a] *Hailang Zhang,*[a] *Qiangchun Liu,*[a]* *and Xiangkai Kong,*[a,c]*

[a] Anhui Province Key Laboratory of Pollutant Sensitive Materials and Environmental Remediation, Huaibei Normal University, Huaibei, Anhui, 235000, P.R. China

[b] School of Chemistry and Chemical Engineering, Nanjing University, Nanjing, Jiangsu, 210023, P.R. China

[c] School of Materials and Physics, China University of Mining and Technology, Xuzhou, Jiangsu, 221116, P.R. China

*Corresponding Author:

*E-mail for X. Kong : xkong@cumt.edu.cn
*E-mail for Q. Liu : qchliu@chnu.edu.cn

Supporting information

Experimental

Materials

Ruthenium acetylacetonate ($Ru(acac)_3$) was purchased from Macklin Chemical Reagent Co., Ltd. Magnesium oxide (MgO), nitric acid (HNO_3), isopropanol and ethanol were purchased from Sinopharm Chemical Reagent Co., Ltd. Deionized water (DI water) was used in all the experiments. All reagents used without any further purification.

Physicochemical characterization

Using a PAN analytical Empyrean X-ray diffractometer with Cu Kα radiation, the crystal structures of the samples were determined by Powder X-ray diffraction (XRD) patterns. Scanning electron microscopy was conducted with a HITACHI REGULUS-8220. Transmission electron microscopy (TEM, JEM-2100F) was employed to analyze the samples' morphologies. An energy-dispersive X-ray spectrometry (EDS, X-Max, Oxford Instruments) attached to the SEM was used for elemental mapping. For additional confirmation of the chemical composition and surface electronic states via high-resolution X-ray photoelectron spectroscopy (XPS, Kratos Axis $Supra^+$). Raman spectra were taken on a via-Reflex, in which the wavelength of the laser is 532 nm. Fourier transform infrared (FTIR) spectra were recorded using a Nicolet iS50 Spectrophotometer (Thermo-Scientific). In situ Raman spectra were recorded on an XPLORA PLUS Raman spectrometer. A homemade Teflon electrochemical cell was used for Raman measurement. The synthesized sample was used as the working electrode. The reference electrode and counter electrode were Hg/HgO and Pt wire, respectively. In order to apply a control potential to the catalyst during the Raman measurement, chronoamperometry was performed in 0.1 M KOH at different potentials. Inductively coupled plasma (ICP) measurements were performed on a Thermo Fisher iCAP 7400.

Electrochemical measurement

All electrochemical experiments were carried out using a standard three-electrode setup on a CHI 760e electrochemical workstation (CH Instruments, Inc.) under ambient conditions. The synthesized catalyst-coated electrode served as the working electrode, while a carbon rod and a Hg/HgO electrode functioned as the counter and reference electrodes, respectively. A catalyst ink was prepared by dispersing 5 mg of the sample and 20 µL of Nafion solution (5 wt%, Aldrich) into 2.5 mL of a water and isopropanol mixture (volume ratio 3:2), followed by 20 minutes of ultrasonication to ensure uniform dispersion. Subsequently, 5 µL of the ink was drop-cast onto a glassy carbon electrode (3 mm diameter) that had been polished beforehand. Electrochemical measurements were conducted in 1.0 M KOH solution, which was defeated by purging with argon prior to hydrogen evolution reaction (HER) tests. All recorded potentials were converted to the reversible hydrogen electrode (RHE) scale. To minimize non-Faradaic contributions, linear sweep voltammetry (LSV) was conducted at a slow scan rate of 5 mV s^{-1}. Electrochemical impedance spectroscopy (EIS) was performed at an overpotential of 50 mV, using a 5 mV amplitude across a frequency range of 100 kHz to 0.05 Hz. The electrochemical double-layer capacitance (Cdl) was estimated by cyclic voltammetry (CV) within the non-Faradaic range (0-0.1 V), using scan rates of 10, 20, 50, 80, and 100 mV s^{-1}. CO stripping experiments were performed by maintaining the electrode at 0.4 V for 600 s in a CO-saturated electrolyte. This was followed by purging with Ar to eliminate dissolved CO, after which CV was applied to oxidize the adsorbed CO species. The catalyst stability was assessed by chronopotentiometry at a constant current density of 10 mA cm^{-2}. Furthermore, HER performance was also evaluated in neutral (1.0 M Na_2SO_4) and acidic (0.5 M H_2SO_4) media, using an Ag/AgCl electrode as the reference. Turnover frequency (TOF) values were estimated under the assumption that all metal atoms are catalytically active, using the equation: TOF = J / (2×F×n), where J is the current density at 50 mV overpotential, F is Faraday's constant (96485.3 C mol^{-1}), the factor 2 corresponds to the two-electron transfer per H_2 molecule, and n is the number of moles of metal atoms determined via CO stripping.

Figures

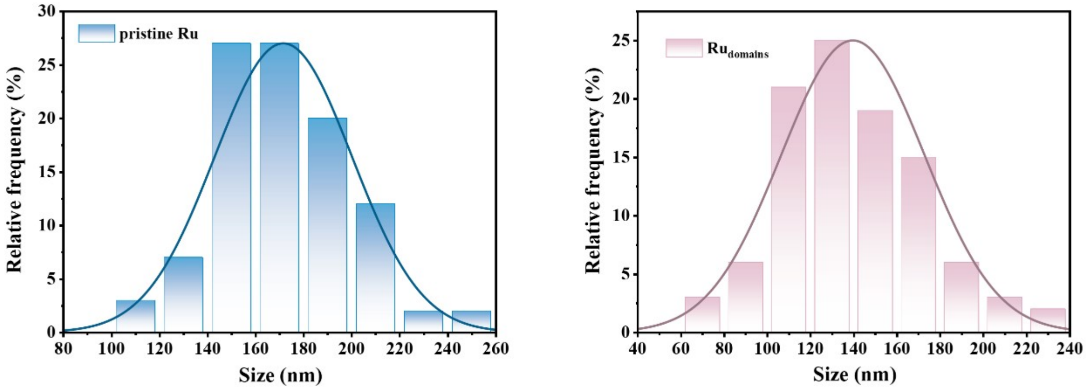

Fig. S1. The Statistical histogram for the size of (a) pristine Ru and (a) Ru$_{domains}$.

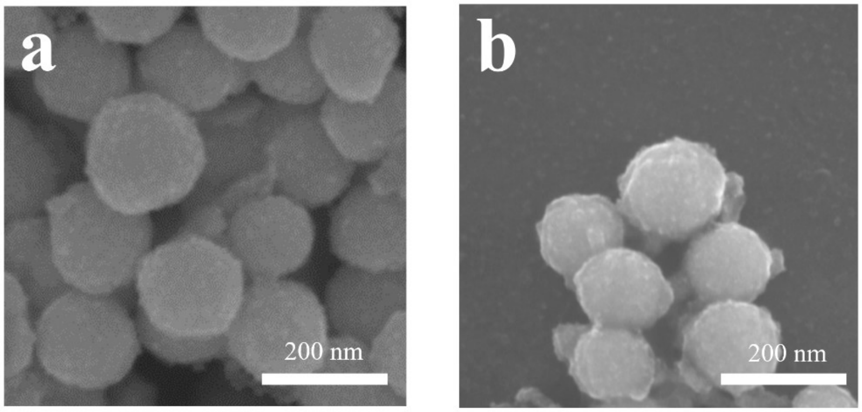

Fig. S2. SEM images of (a) Ru$_{domains}$-1 and (b) Ru$_{domains}$-2.

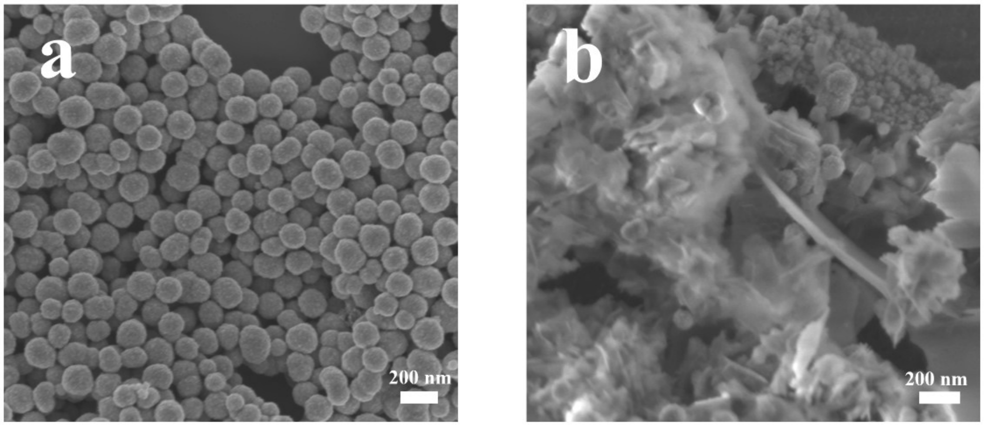

Fig. S3. SEM images of (a) pristine Ru and (b) $Ru_{domains}$ before acid treatment.

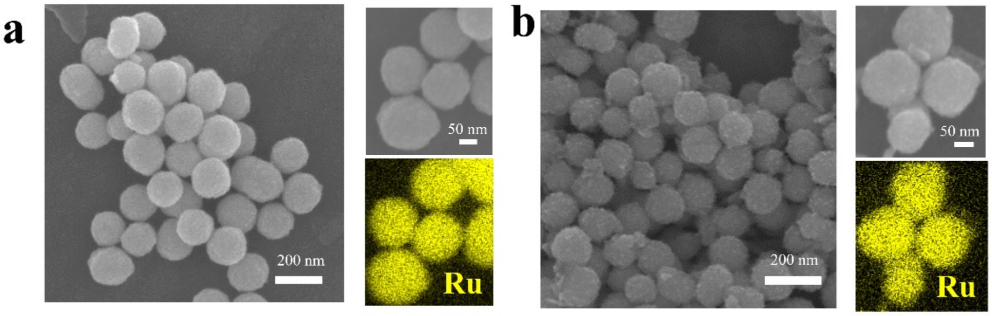

Fig. S4. Elemental mapping of (a) pristine Ru and (b) $Ru_{domains}$.

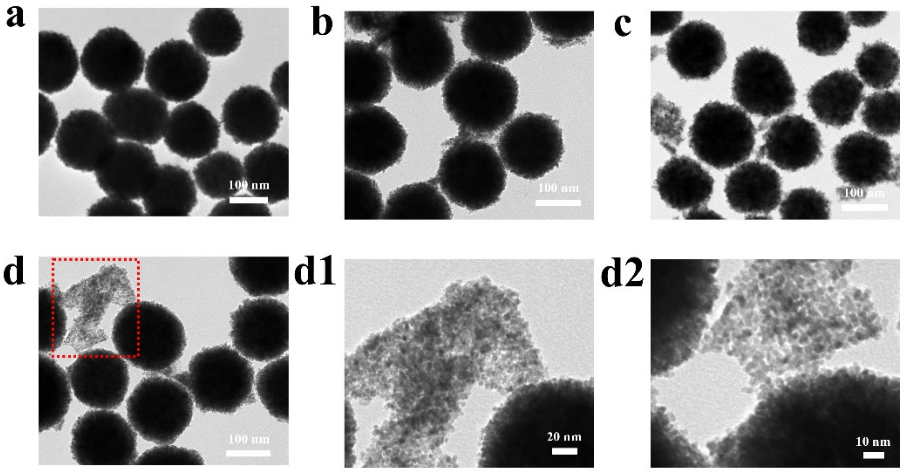

Fig. S5. TEM images of (a) pristine Ru, (b) $Ru_{domains}$-1 , (c) $Ru_{domains}$-2, (d, d1, d2) $Ru_{domains}$.

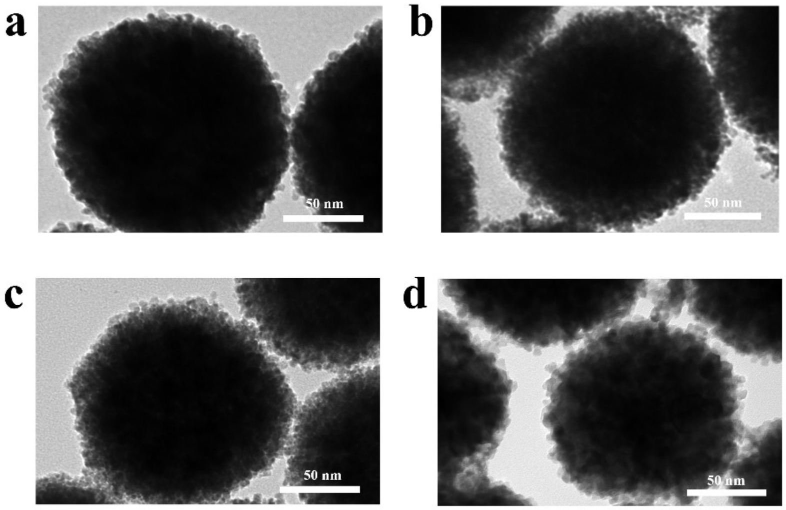

Fig. S6. TEM images of (a) pristine Ru, (b) $Ru_{domains}$-1 , (c) $Ru_{domains}$, (d) $Ru_{domains}$-2.

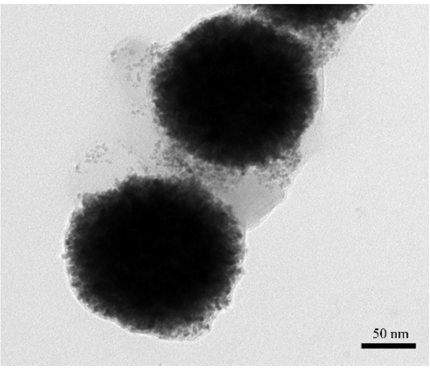

Fig. S7. TEM images of D-$Ru_{domains}$.

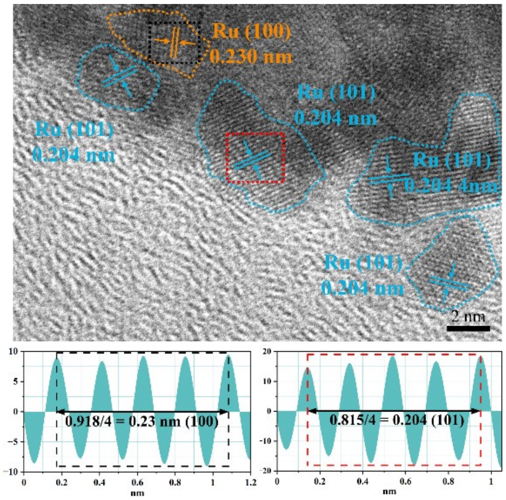

Fig. S8. HRTEM image of $Ru_{domains}$-1, with corresponding intensity profiles of the selected area.

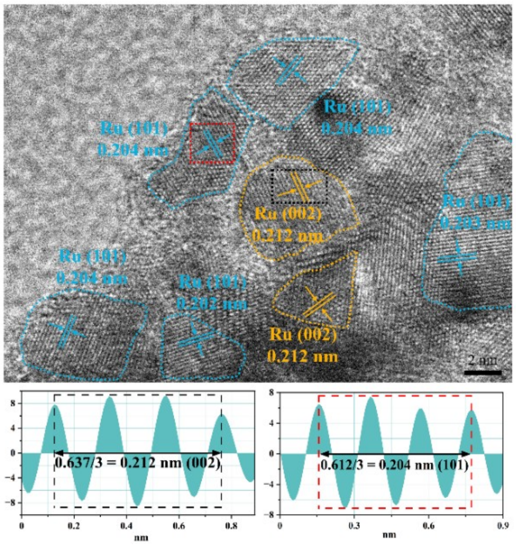

Fig. S9. HRTEM image of $Ru_{domains}$-2, with corresponding intensity profiles of the selected area.

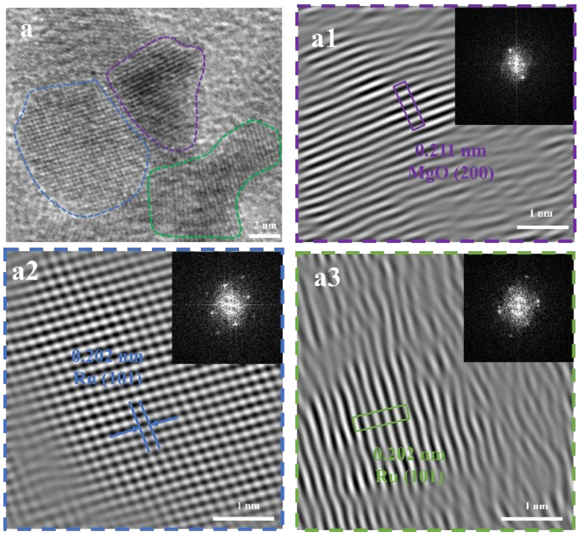

Fig. S10. HRTEM image of D-$Ru_{domains}$, FFT and IFFT images corresponding intensity profiles of the selected area.

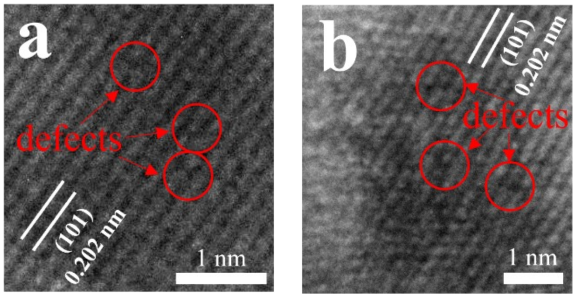

Fig. S11. HRTEM image of $Ru_{domains}$.

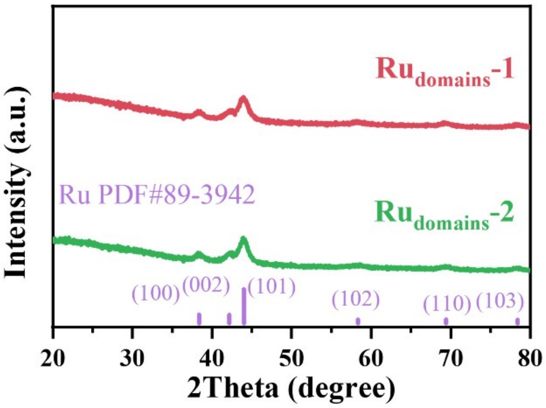

Fig. S12. XRD patterns of Ru$_{domains}$-1 and Ru$_{domains}$-2.

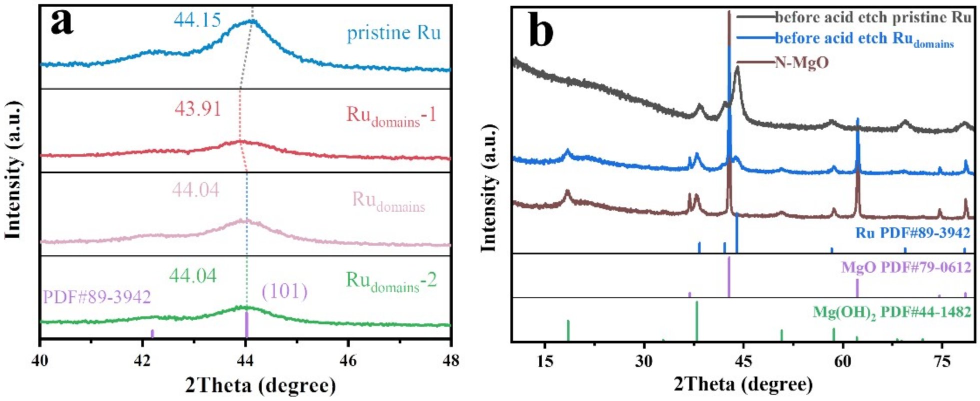

Fig. S13. (a) XRD patterns, (b) XRD patterns of pristine Ru, Ru$_{domains}$ before nitric acid cleaning and N-MgO.

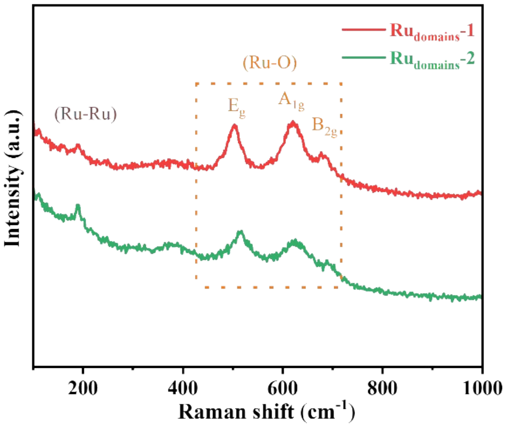

Fig. S14. Raman spectra of Ru$_{domains}$-1 and Ru$_{domains}$-2.

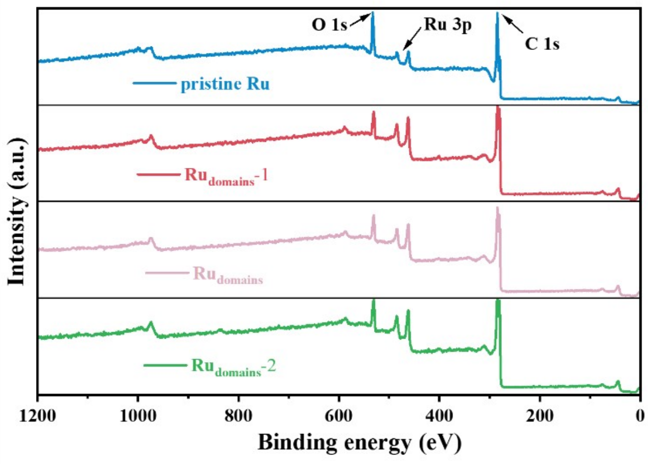

Fig. S15. The measured XPS survey spectra for these samples.

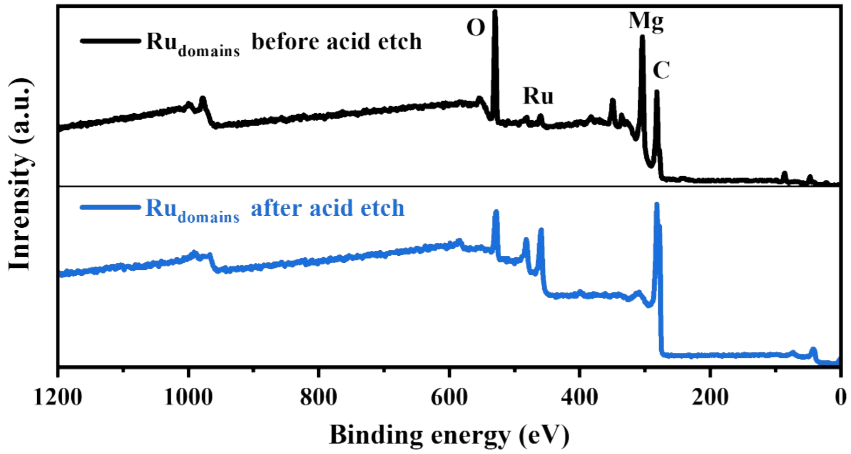

Fig. S16. XPS survey spectra of $Ru_{domains}$ before and after acid etch.

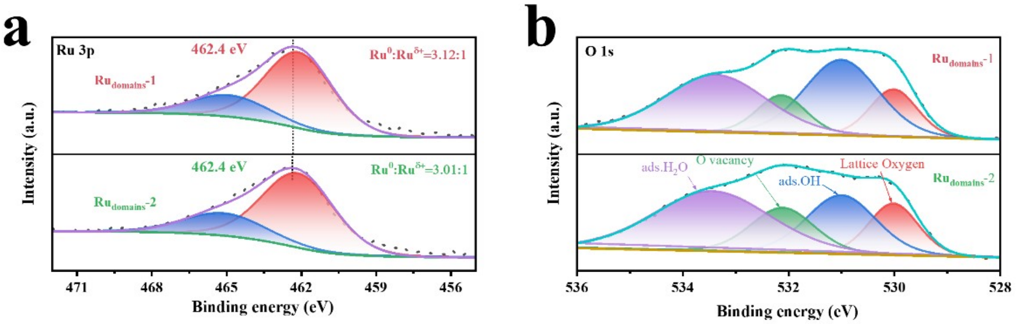

Fig. S17. XPS spectra of $Ru_{domains}$-1 and $Ru_{domains}$-2 (a) Ru 3p, (b) O1s.

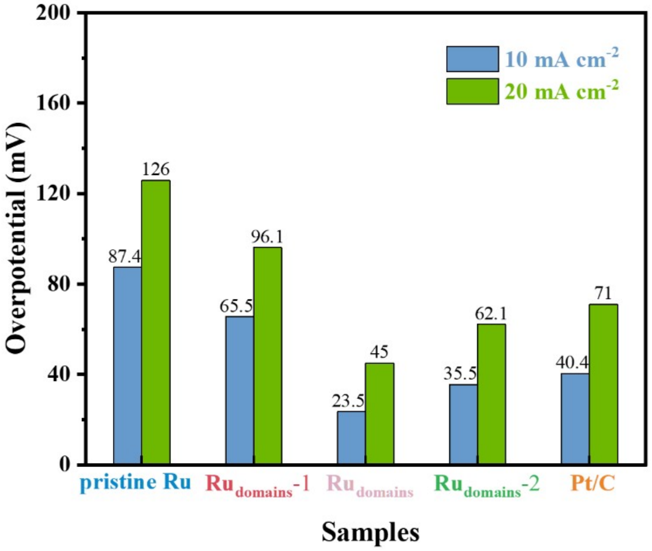

Fig. S18. Overpotential comparison histogram of pristine Ru, Ru$_{domains}$-1, Ru$_{domains}$, Ru$_{domains}$-2 and commercial Pt/C catalysts under 10 and 20 mA cm^{-2}.

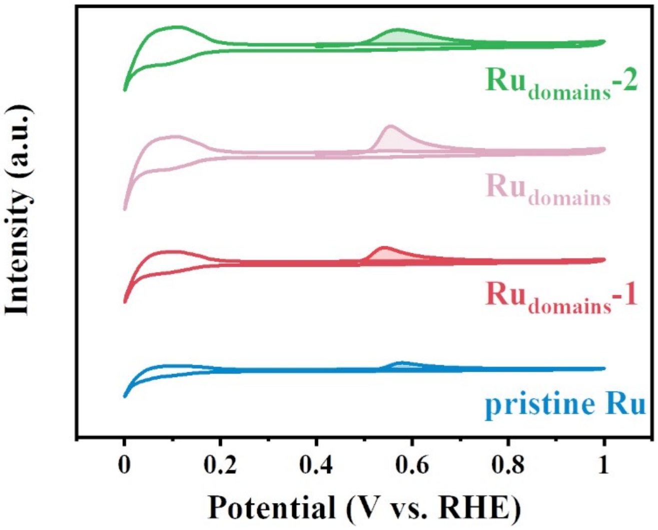

Fig. S19. CO stripping measurement on these samples.

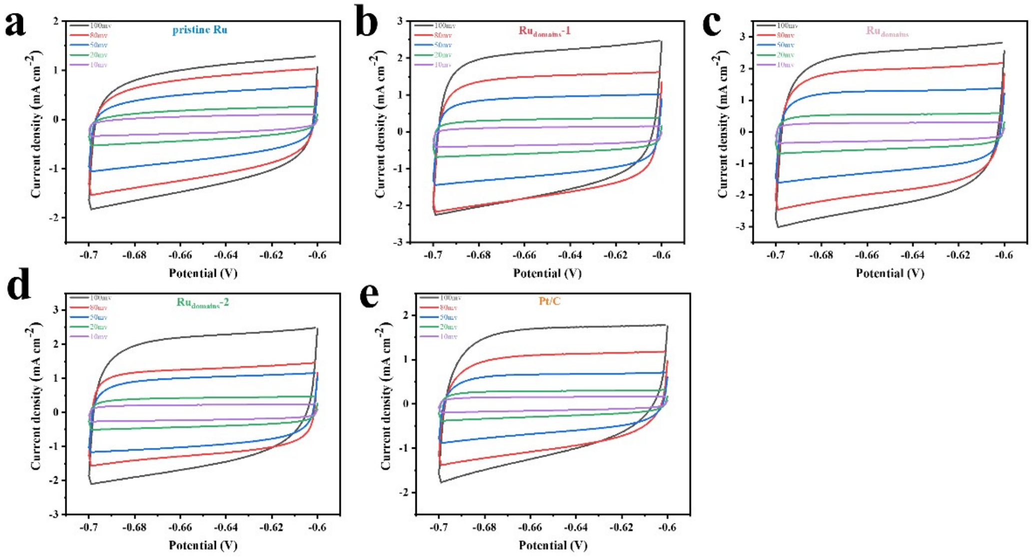

Fig. S20. The corresponding CV curves of Ru, Ru$_{domains}$-1, Ru$_{domains}$, Ru$_{domains}$-2 and commercial Pt/C catalysts.

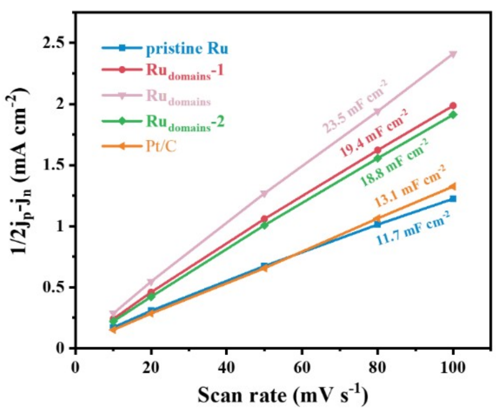

Fig. S21. DLC measurement in 1.0 M KOH of Ru, Ru$_{domains}$-1, Ru$_{domains}$, Ru$_{domains}$-2 and commercial Pt/C catalysts.

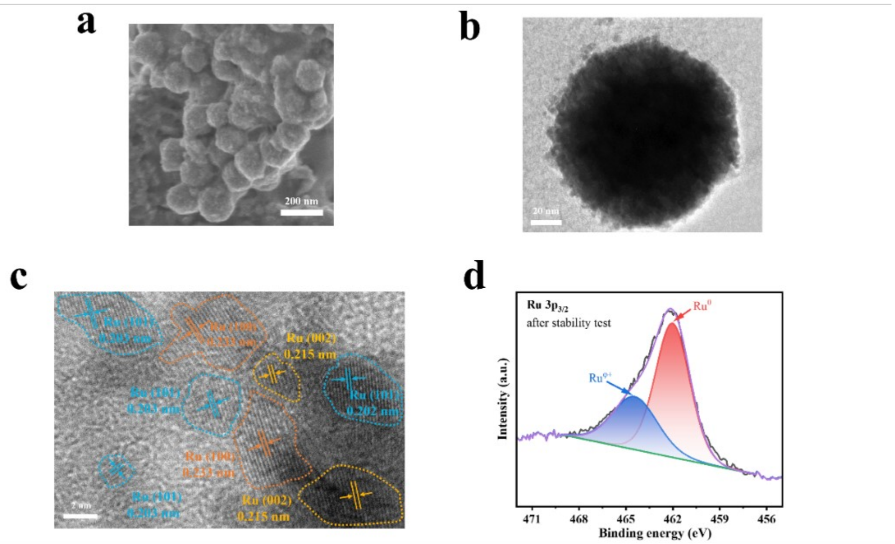

Fig. S22. $Ru_{domains}$ after the electrochemical durability evaluation: (a) SEM image, (b) TEM image, (c) HRTEM image and (d) Ru 3p of XPS.

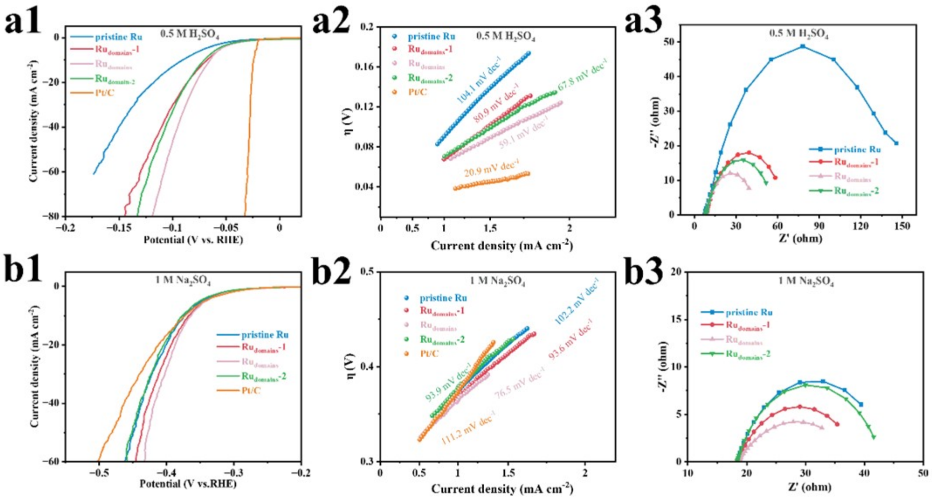

Fig. S23. LSV curves, Tafel plots, EIS spectra of these catalysts in (a1-3) 0.5 M H_2SO_4 and (b1-3) 1 M Na_2SO_4 electrolytes.

Tables

Table S1. ICP measurements of $Ru_{domains}$.

Catalysis	Element	concentration (ug/ml)	Mass fraction (%)
$Ru_{domains}$	Ru	0.135397892	100%

	Mg	0	0%

Table S2. HER performance comparison of $Ru_{domains}$ with recently reported Ru-based catalysts.

Catalyst	**Electrolyte**	**η_{10} (mV)**	**Tafel plots(mV dec^{-1})**	**Reference**
$Ru_{domains}$	1M KOH	23.5	34.4	This work
RuCo@NC	1M KOH	28	31	[1]
Ru@CN	1M KOH	32	53	[2]
Ru-Cu-2	1M KOH	33	37	[3]
NiO/Ru@PNS	1M KOH	39	75	[4]
Ru/NC-400	1M KOH	39	49	[5]
Ru-MoS_2/CC	1M KOH	41	114	[6]
Ru-G/CC	1M KOH	40	76	[7]
Ru@1T-MoS_2-Mxene	1M KOH	42	38	[8]
Co@RuCo	1M KOH	46	50	[9]
Ru-$Mo_2Ti_2C_3$	1M KOH	47	49	[10]
Ru/S–Ni_2P	1M KOH	49	43.1	[11]
Au-Ru NWs	1M KOH	50	30.8	[12]
Ru@2H-MoS_2	1M KOH	51	64.9	[13]
RuP_2@NPC	1M KOH	52	69	[14]
$Ni_{1.5}Co_{1.4}P$@Ru	1M KOH	52	50	[15]
Ru/Co_4N-CoF_2	1M KOH	53	114.1	[16]
Sr_2RuO_4	1M KOH	61	51	[17]
Ru/TiO_2-VO@C-15	1M KOH	64	58	[18]
Ru/C_3N_4/C	1M KOH	79	49	[19]
$Cu_{2-x}S$/Ru	1M KOH	82	48	[20]

Reference

1. J. Su, Y. Yang, G. Xia, J. Chen, P. Jiang and Q. Chen, Ruthenium-cobalt nanoalloys encapsulated in nitrogen-doped graphene as active electrocatalysts for producing hydrogen in alkaline media, *Nat. Commun.*, 2017, **8**, 14969.
2. J. Wang, Z. Wei, S. Mao, H. Li and Y. Wang, Highly uniform Ru nanoparticles over N-doped carbon: pH and temperature-universal hydrogen release from water reduction, *Energy Environ. Sci.*, 2018, **11**, 800-806.
3. H. Huang, H. Jung, S. Li, S. Kim, J. W. Han and J. Lee, Activation of inert copper for significantly enhanced hydrogen evolution behaviors by trace ruthenium doping, *Nano Energy*, 2022, **92**, 106763.
4. C. Zhong, Q. Zhou, S. Li, L. Cao, J. Li, Z. Shen, H. Ma, J. Liu, M. Lu and H. Zhang, Enhanced synergistic catalysis by a novel triple-phase interface design of NiO/Ru@Ni for the hydrogen evolution reaction, *J. Mater. Chem. A,* 2019, **7**, 2344-2350.
5. M. Lao, G. Zhao, P. Li, T. Ma, Y. Jiang, H. Pan, S. X. Dou and W. Sun, Manipulating the Coordination Chemistry of Ru-N(O)-C Moieties for Fast Alkaline Hydrogen Evolution Kinetics, *Adv. Funct. Mater.*, 2021, **31**, 2100698.
6. D. Wang, Q. Li, C. Han, Z. Xing and X. Yang, Single-atom ruthenium based catalyst for enhanced hydrogen evolution, *Appl. Catal., B*, 2019, **249**, 91-97.
7. M. You, X. Du, X. Hou, Z. Wang, Y. Zhou, H. Ji, L. Zhang, Z. Zhang, S. Yi and D. Chen, In-situ growth of ruthenium-based nanostructure on carbon cloth for superior electrocatalytic activity towards HER and OER, *Appl. Catal., B*, 2022, **317**, 121729.
8. G. Li, T. Sun, H. J. Niu, Y. Yan, T. Liu, S. Jiang, Q. Yang, W. Zhou and L. Guo, Triple Interface Optimization of Ru-based Electrocatalyst with Enhanced Activity and Stability for Hydrogen Evolution Reaction, *Adv. Funct. Mater.*, 2023, **33**, 2212514.
9. H. Huang, H. Jung, C.-Y. Park, S. Kim, A. Lee, H. Jun, J. Choi, J. W. Han and J. Lee, Surface conversion derived core-shell nanostructures of Co particles@RuCo alloy for superior hydrogen evolution in alkali and seawater, *Appl. Catal., B*, 2022, **315**, 121554.
10. X. Liu, F. Xie, Q. Xi, Y. Wang, Y. Wang, H. Li, R. Li, C. Fan, J. Liu and J. Wang, H_3O^+ assisted hydrogen spillover over Ru-$Mo_2Ti_2C_3$ for efficient alkaline hydrogen evolution, *J. Colloid Interface Sci.*, 2025, **694**, 137738.
11. J. Chen, C. Chen, Y. Chen, H. Wang, S. Mao and Y. Wang, Improving alkaline hydrogen evolution reaction kinetics on molybdenum carbide: Introducing Ru dopant, *J. Catal.*, 2020, **392**, 313-321.
12. Q. Lu, A.-L. Wang, Y. Gong, W. Hao, H. Cheng, J. Chen, B. Li, N. Yang, W. Niu, J. Wang, Y. Yu, X. Zhang, Y. Chen, Z. Fan, X.-J. Wu, J. Chen, J. Luo, S. Li, L. Gu and H. Zhang, Crystal phase-based epitaxial growth of hybrid noble metal nanostructures on 4H/fcc Au nanowires, *Nat. Chem.*, 2018, **10**, 456-461.
13. J. Wang, W. Fang, Y. Hu, Y. Zhang, J. Dang, Y. Wu, B. Chen, H. Zhao and Z. Li, Single atom Ru doping 2H-MoS_2 as highly efficient hydrogen evolution reaction electrocatalyst in a wide pH range, *Appl. Catal., B*, 2021, **298**, 120490.
14. Z. Pu, I. S. Amiinu, Z. Kou, W. Li and S. Mu, RuP_2 -Based Catalysts with Platinum-like Activity and Higher Durability for the Hydrogen Evolution Reaction at All pH Values,

Angew. Chem. Int. Ed., 2017, **56**, 11559-11564.

15. S. Liu, Q. Liu, Y. Lv, B. Chen, Q. Zhou, L. Wang, Q. Zheng, C. Che and C. Chen, Ru decorated with NiCoP: an efficient and durable hydrogen evolution reaction electrocatalyst in both acidic and alkaline conditions, *Chem. Commun.*, 2017, **53**, 13153-13156.
16. S. Zhou, H. Jang, Q. Qin, Z. Li, M. Gyu Kim, X. Ji, X. Liu and J. Cho, Ru atom-modified Co_4N-CoF_2 heterojunction catalyst for high-performance alkaline hydrogen evolution, *Chem. Eng. J.,* 2021, **414**, 128865.
17. Y. Zhu, H. A. Tahini, Z. Hu, J. Dai, Y. Chen, H. Sun, W. Zhou, M. Liu, S. C. Smith, H. Wang and Z. Shao, Unusual synergistic effect in layered Ruddlesden-Popper oxide enables ultrafast hydrogen evolution, *Nat. Commun.*, 2019, **10**, 149.
18. Z. Wei, Z. Zhao, J. Wang, Q. Zhou, C. Zhao, Z. Yao and J. Wang, Oxygen-deficient TiO_2 and carbon coupling synergistically boost the activity of Ru nanoparticles for the alkaline hydrogen evolution reaction, *J. Mater. Chem. A,* 2021, **9**, 10160-10168.
19. Y. Zheng, Y. Jiao, Y. Zhu, L. H. Li, Y. Han, Y. Chen, M. Jaroniec and S.-Z. Qiao, High Electrocatalytic Hydrogen Evolution Activity of an Anomalous Ruthenium Catalyst, *J. Am. Chem. Soc.*, 2016, **138**, 16174-16181.
20. D. Yoon, J. Lee, B. Seo, B. Kim, H. Baik, S. H. Joo and K. Lee, Cactus-Like Hollow $Cu_{2-x}S$@Ru Nanoplates as Excellent and Robust Electrocatalysts for the Alkaline Hydrogen Evolution Reaction, *Small*, 2017, **13**, 1700052.